Structure, Magnetism and Photomagnetism of Mixed - Ligand Tris(pyrazolyl)methane Iron(II) Spin Crossover Compounds.

Boujemaa Moubaraki, [a] Ben A. Leita, [a] Gregory J. Halder,[b] Stuart R. Batten,[a] Paul Jensen, [a] Jonathan P. Smith,[a] John D. Cashion,[c] Cameron J. Kepert,[b] Jean-François Létard[d] and Keith S Murray.[a] *

ELECTRONIC SUPPLEMENTARY DATA

Contact keith.murray@sci.monash.edu.au

CONTENTS

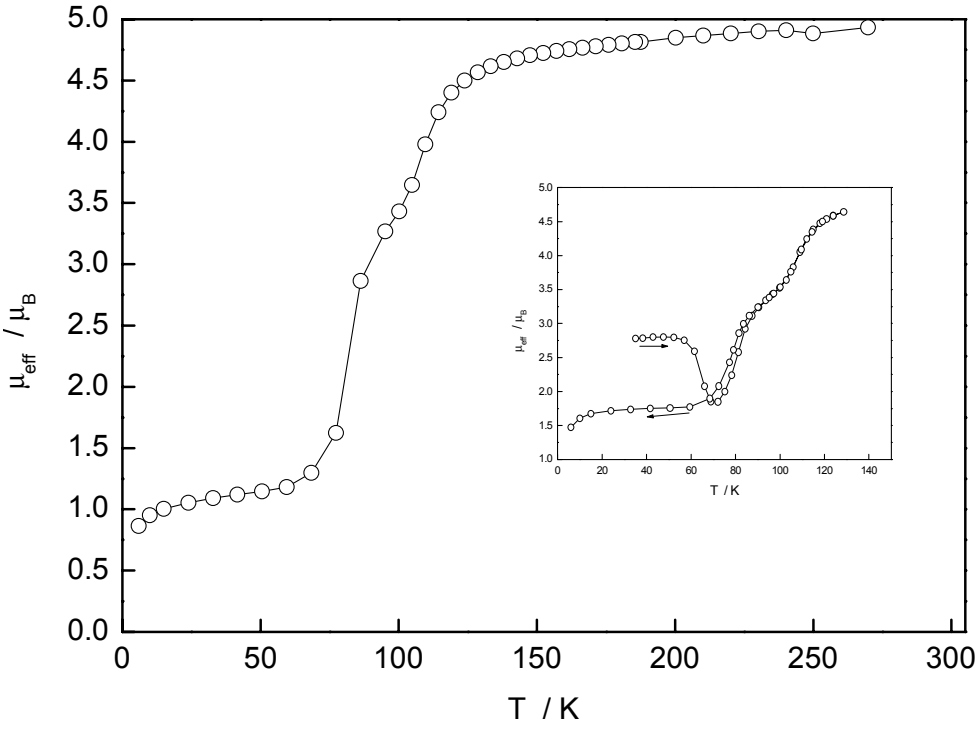

Fig. S1 Magnetic properties of freshly prepared [Fe(dmtpm)(4mtpm)]$(BF_4)_2$.1.5MeCN, **2**. The main plot is as in Fig. 4. The inset shows a more detailed temperature variation around the spin transitions and shows trapping of the metastable HS state when the sample was quench cooled to 35 K before slowly warming to 130 K and then cooled again, slowly.

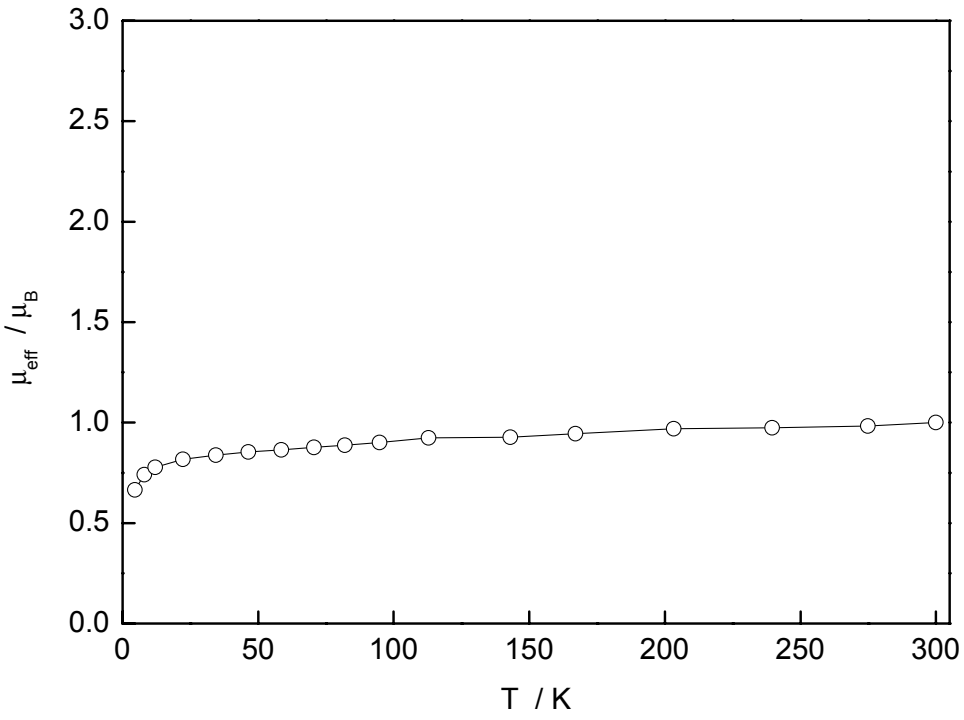

Fig S2 Plot of magnetic moment, μ_{eff}, vs temperature for $[Fe((py)_3CH)(3,5\text{-}Me_2pz)_3CH)][BF_4]_2$, **4**, showing LS behaviour over the whole temperature range.

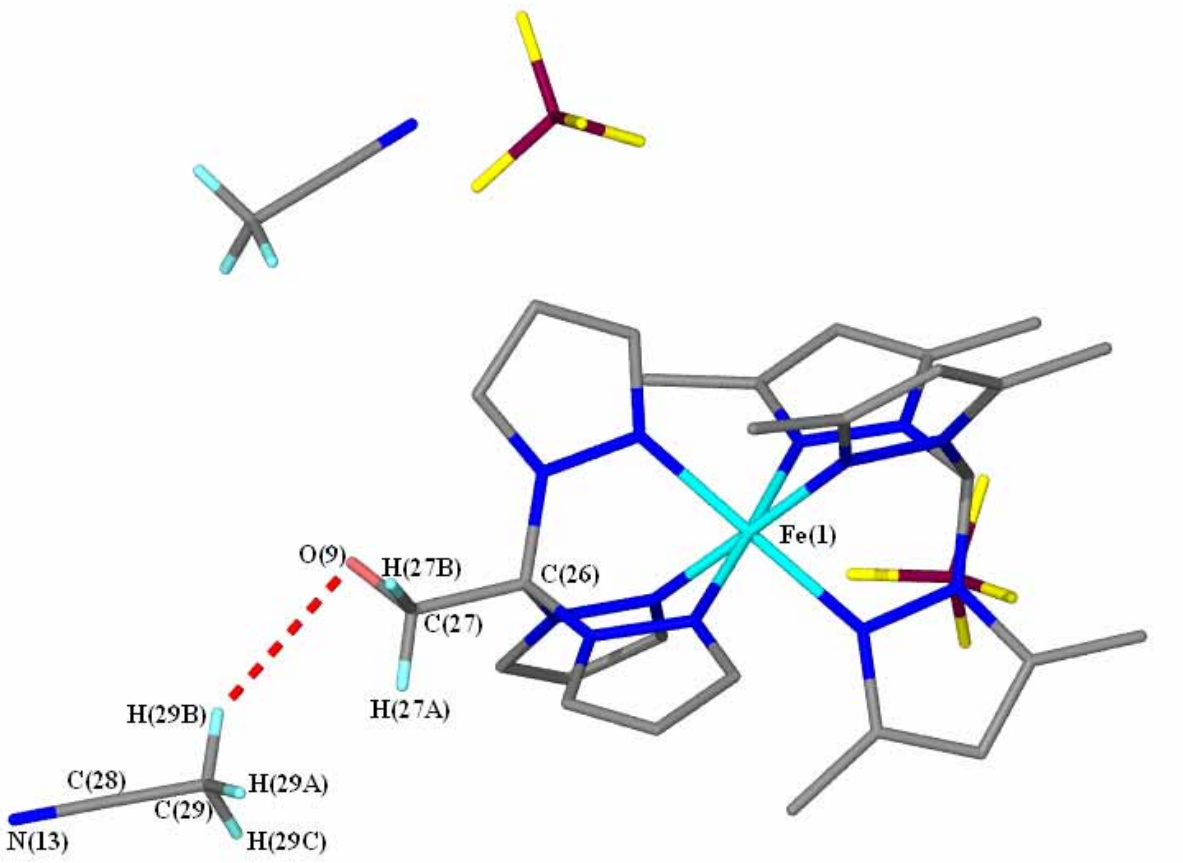

Fig. S3 Interaction of the $(pz)_3C(CH_2OH)$ ligand atom O(9) with one of the lattice MeCN molecules in **3**, at 123.

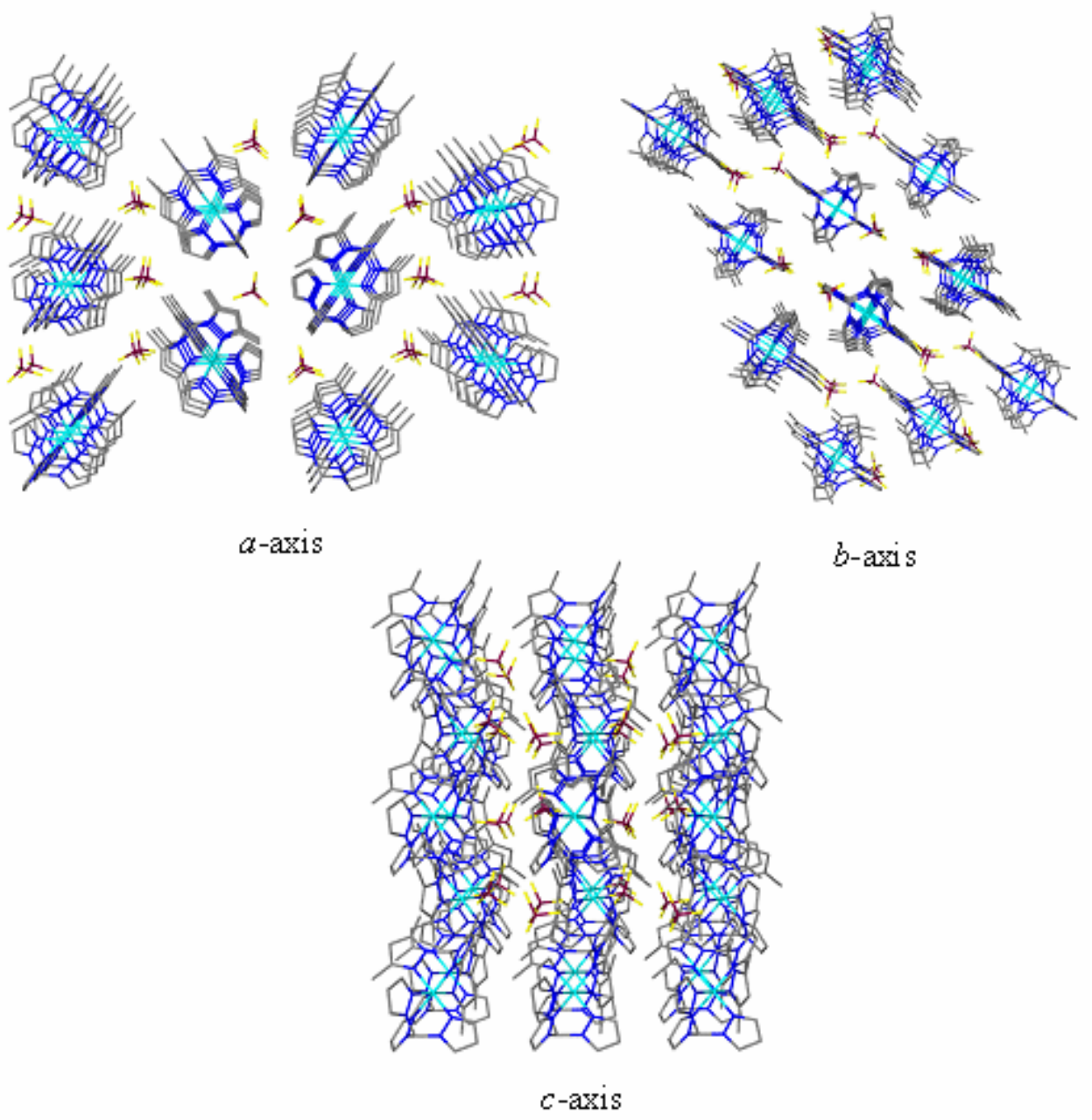

Fig. S4 Crystal packing diagram of $[Fe((pz)_3CH)((3,5\text{-}Me_2pz)_3CH)][BF_4]_2$, polymorph **1a,** viewed down the *a*-, *b*- and *c*-axes, (solved at 123 K).

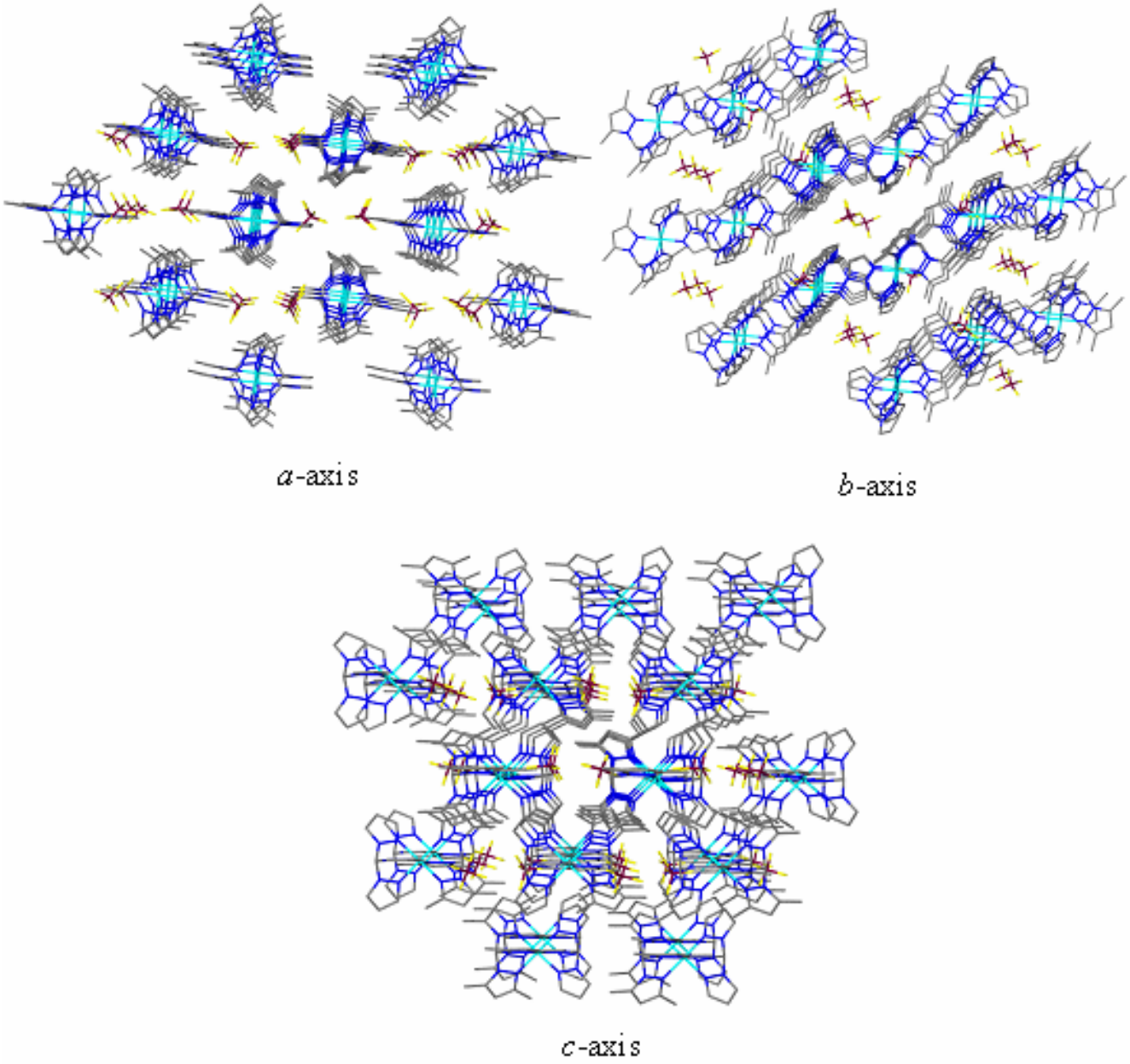

Fig. S5 Crystal packing for polymorph **1b** viewed down the *a*-, *b*- and *c*-axes, at 123 K.

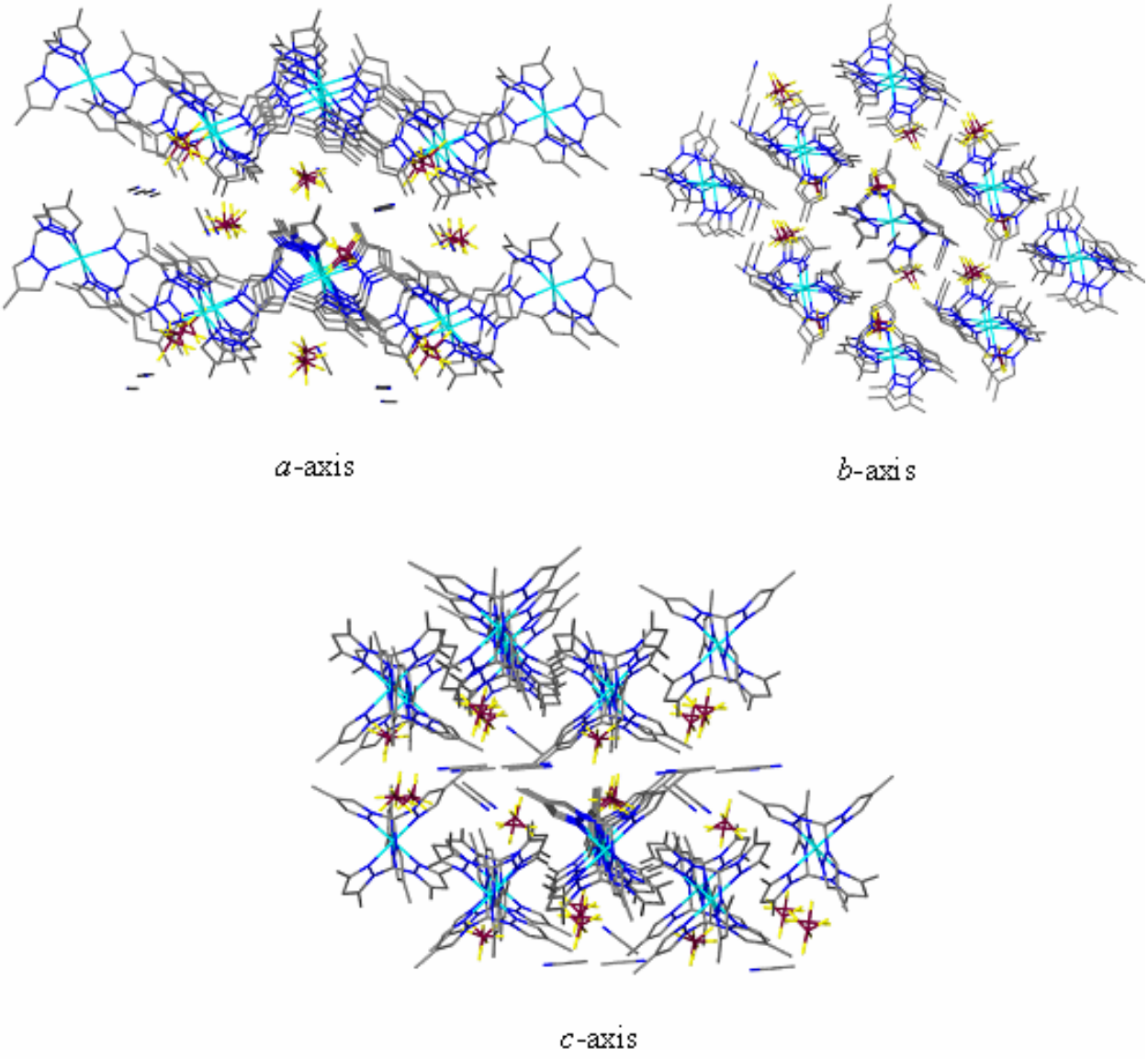

Fig. S6. Crystal packing diagram of [Fe((4-Mepz)$_3$CH)((3,5-Me$_2$pz)$_3$CH)](BF$_4$]$_2$.1.5MeCN , **2**, viewed down the *a*-, *b*- and *c*-axes, at 25 K (25ss).

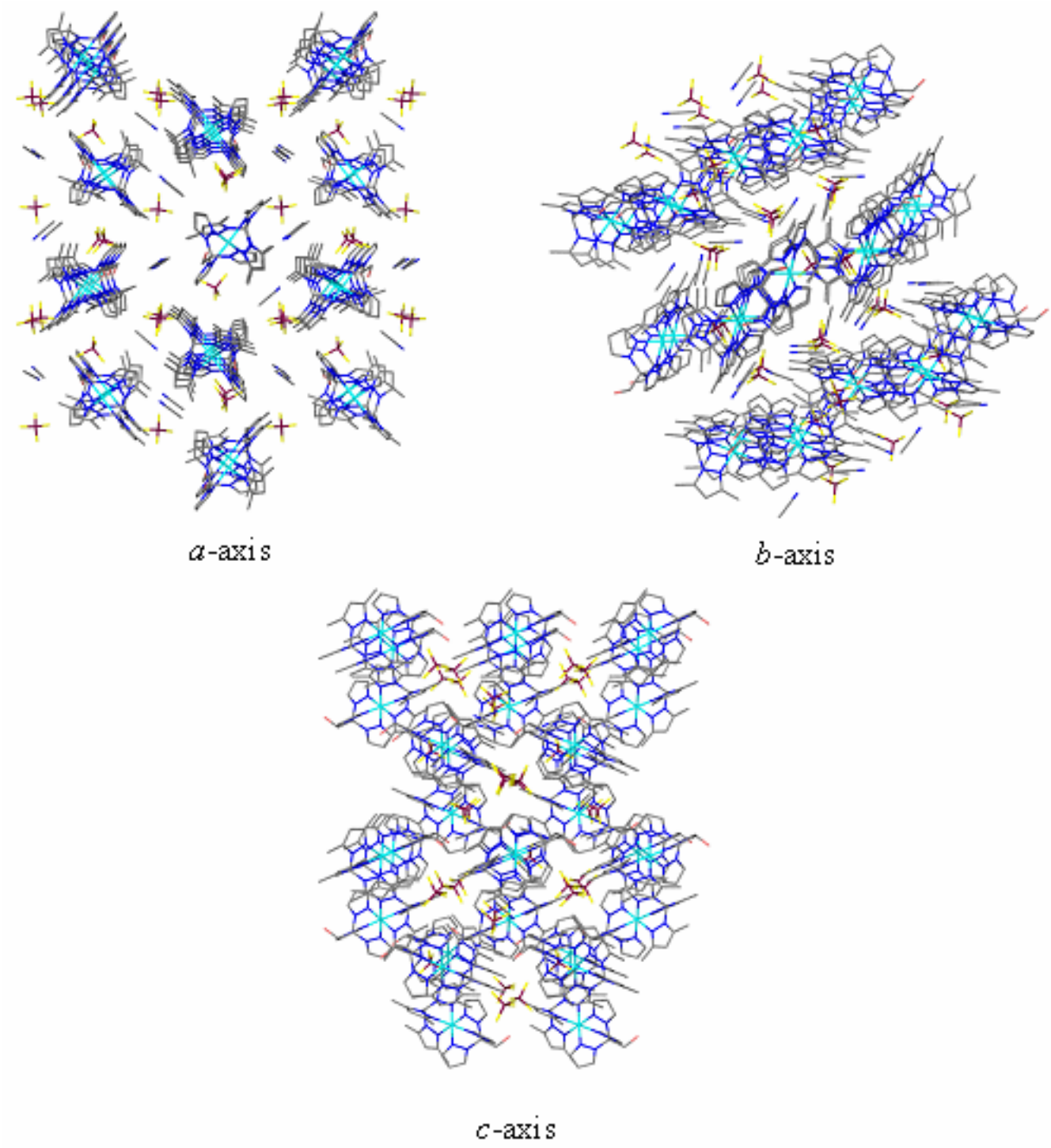

Fig. S7 Crystal packing diagram of $[Fe((pz)_3CCH_2OH)((3,5\text{-}Me_2pz)_3CH)][BF_4]_2.2MeCN$, **3,** viewed down the *a*-, *b*- and *c*-axes, (solved at 123 K).

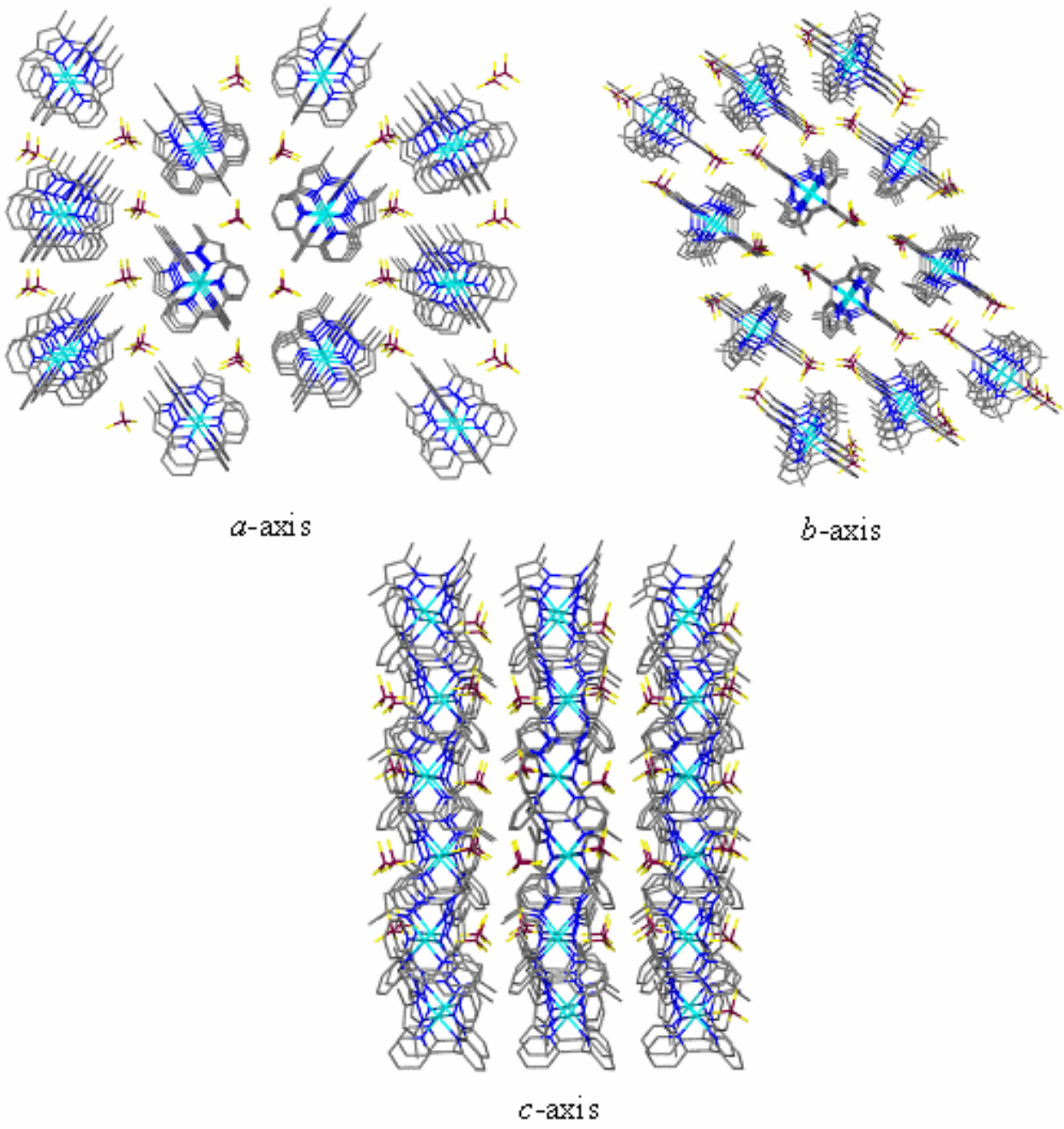

Fig. S8 Packing diagram of $[Fe((py)_3CH)(3,5\text{-}Me_2pz)_3CH)][BF_4]_2$, **4**, viewed down the *a*-, *b*- and *c*-axes, (solved at 123 K).

Fig. S9 Temperature dependence of the unit cell axes for **1b**.

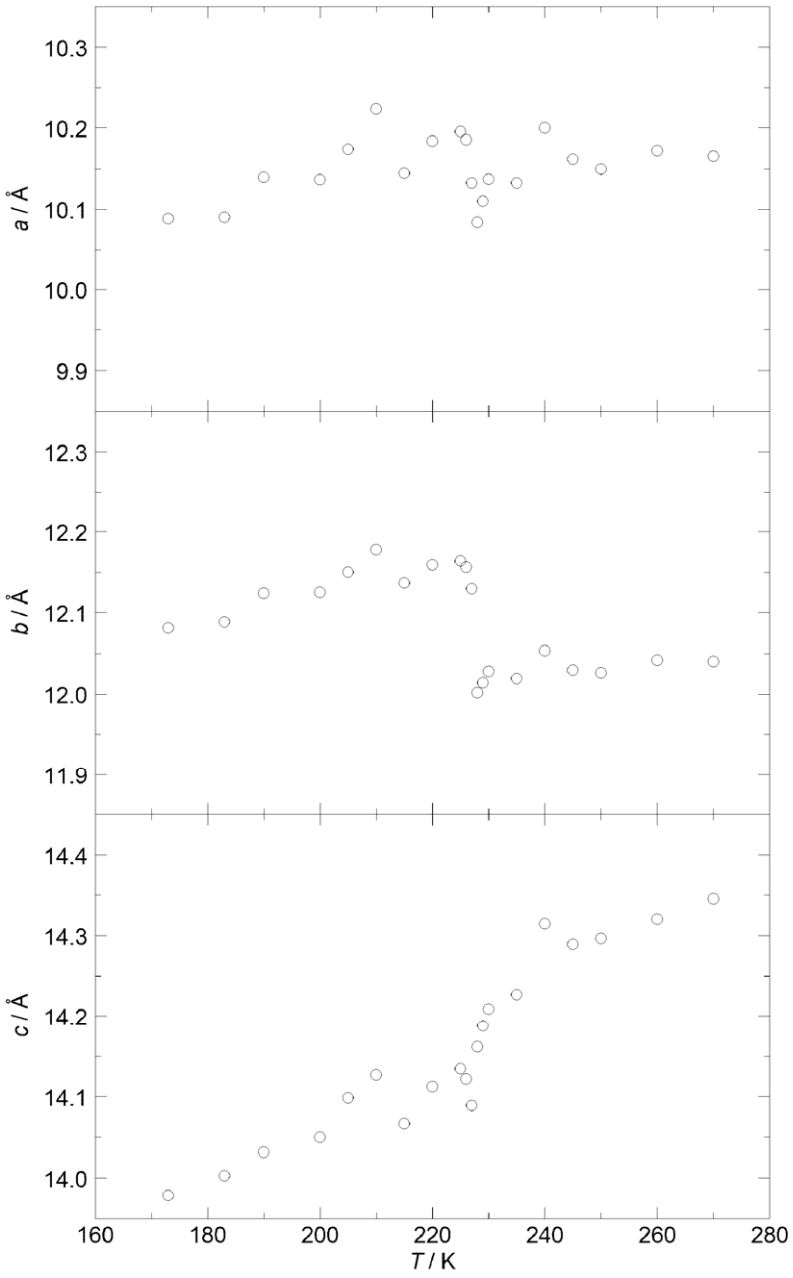

Fig. S10 Temperature dependence of the unit cell angles for **1b**.

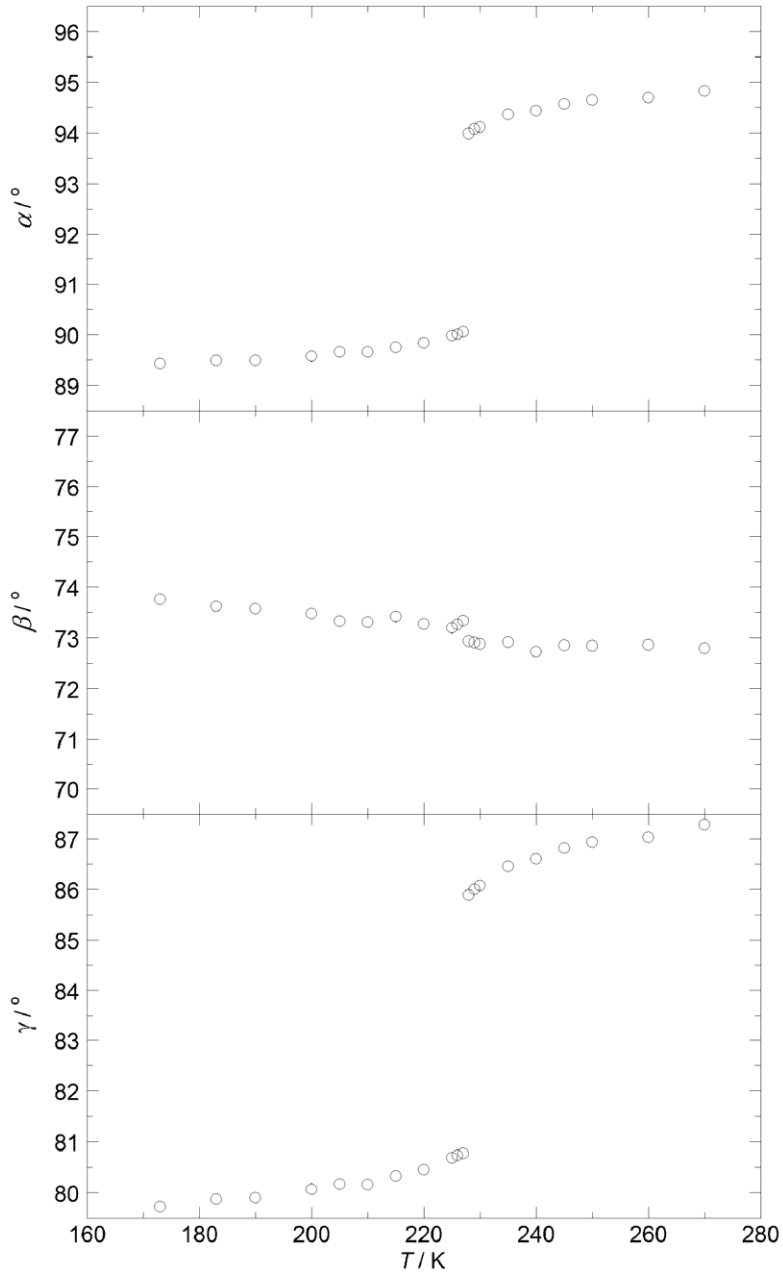

Fig. S11 Temperature dependence of the unit cell volume for **1b**.

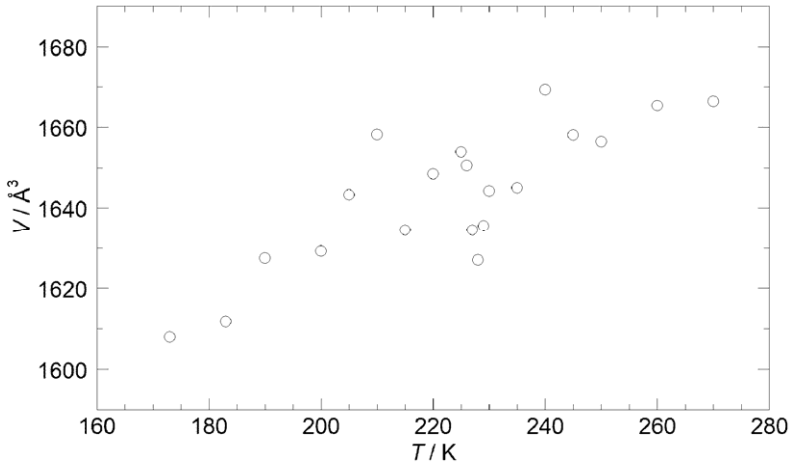

Fig. S12 Temperature dependence of the unit cell axes for **2** following quench-cooling to 25 K (open circles) and on slow-cooling from 140 K (filled triangles).

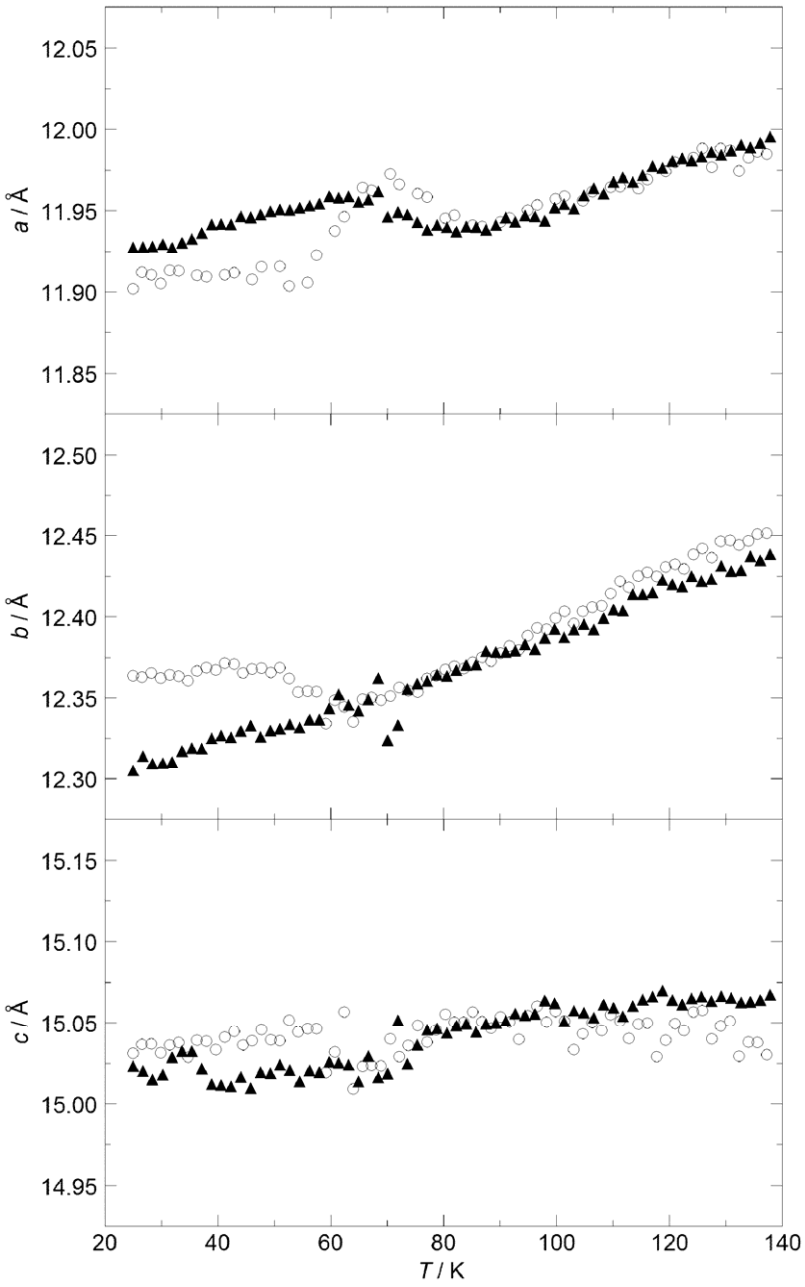

Fig. S13 Temperature dependence of the unit cell angles for **2** following quench-cooling to 25 K (open circles) and on slow-cooling from 140 K (filled triangles).

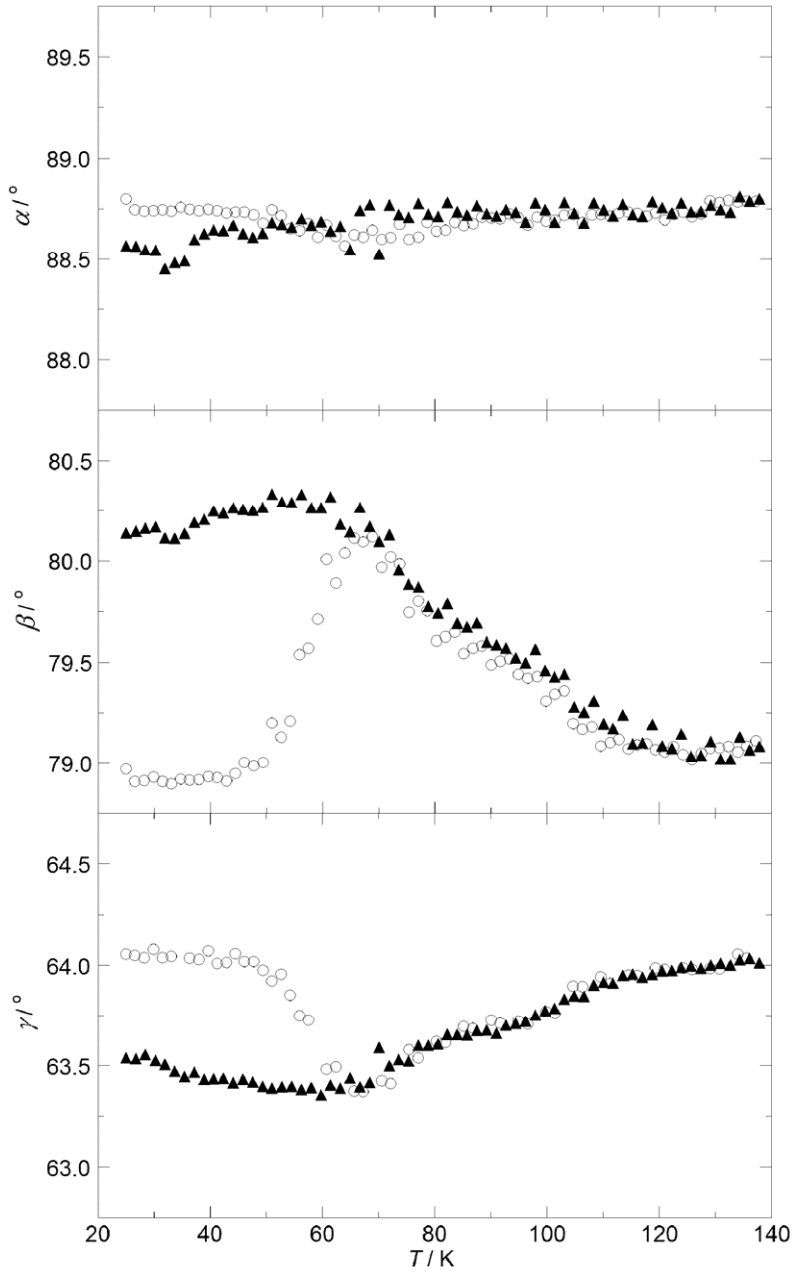

Fig. S14 Temperature dependence of the unit cell volume for **2** following quench-cooling to 25 K (open circles) and on slow-cooling from 140 K (filled triangles).

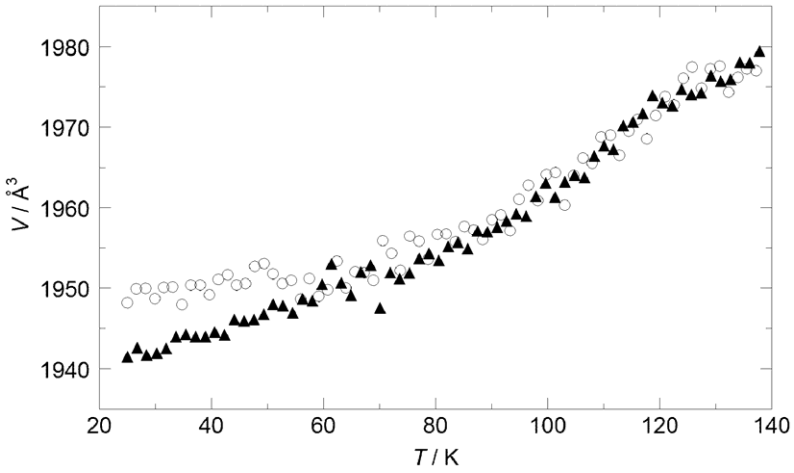

Fig S15 Plots of observed T(LIESST) and T(1/2)values for a data bank of fifty seven Fe(II) spin crossover compounds (see ref. 6 and 12). The solid lines show the relationship T(LIESST) = T_O – 0.3$T_{1/2}$ for the values of T_O shown. Point 57, on the T_O = 100 K line, is for complex **2**. Typical modes of chelation are shown on the top left, including the bis-meridional tridentate complexes with T_O = 150 K (see text).